

Research

Inhibition of PDK modulates radiotherapy resistance in gastric cancer

Qi Zhang³ · Wanjia Qiao² · Xiaoyu Liu² · Jun Lu³ · Farooq Benish² · Shuping Li⁴ · Xiaojun Liu^{1,4}

Received: 25 February 2025 / Accepted: 9 May 2025

Published online: 23 May 2025

© The Author(s) 2025 **OPEN****Abstract**

To explore the effect of sodium dichloroacetate (DCA), a pyruvate dehydrogenase kinase (PDK) inhibitor, on the progression of gastric cancer and resistance to radiotherapy, we analyzed histopathological microarrays from 60 gastric cancer and paracancerous tissues to determine PDK expression and its prognostic significance. 5-Ethynyl-2'-deoxyuridine (EdU) incorporation assay and Transwell migration assay were used to investigate the effects of PDK inhibition on gastric cancer cell proliferation and migration. Flow cytometry revealed that PDK inhibition promoted apoptosis and induced G1 phase cell cycle arrest. Colony formation assay combined with radiation was performed to calculate radiobiological parameters, while Western blot detected the expression of phosphorylated histone H2AX (γ -H2AX), a DNA double-strand break marker. Reactive oxygen species (ROS) generation was measured using the fluorescent probe 2',7'-dichlorodihydrofluorescein diacetate (DCFH-DA). Our results showed that PDK was highly expressed in gastric cancer tissues and correlated with poor patient prognosis. PDK inhibition suppressed proliferation and migration of gastric cancer cells, promoted apoptosis and G1 phase arrest, and enhanced γ -H2AX accumulation and ROS generation, thereby increasing radiosensitivity. These findings demonstrate that targeting PDK inhibits gastric cancer progression and sensitizes tumor cells to radiotherapy.

Keywords Gastric cancer · DCA · PDK · Glycolysis · Radiotherapy resistance**1 Introduction**

In recent years, less than 25% of all patients diagnosed with gastric cancer are in the early stage of gastric cancer, and the survival rate of patients with progressive gastric cancer is still low, with most of them having a 5-year overall survival rate of less than 30% [1]. Radiotherapy is one of the important treatments for gastric cancer, especially gastroesophageal union cancer [2]. However, some gastric cancer patients are resistant to radiotherapy, which affects the local control and long-term survival of gastric cancer [3].

Qi Zhang, Wanjia Qiao, Xiaoyu Liu and Jun Lu have contributed to this work equally.**Supplementary Information** The online version contains supplementary material available at <https://doi.org/10.1007/s12672-025-02635-8>.

✉ Shuping Li, 13321203330@189.cn; ✉ Xiaojun Liu, lxjmail2008@126.com; Qi Zhang, zq570899139@163.com; Xiaoyu Liu, 17793173351@163.com | ¹Key Laboratory of Gastrointestinal Tumor Diagnosis and Treatment, National Health and Wellness Commission, Lanzhou 730000, Gansu, China. ²Lanzhou University, Lanzhou 730000, Gansu, China. ³Xi'an International Medical Center Hospital, Xian 710018, Shanxi, China. ⁴Lanzhou University Third Clinical Medical College, No. 204, Donggang West Road, Chengguan District, Lanzhou 730000, Gansu, China.



Most tumor cells preferentially undergo aerobic glycolysis (Warburg effect) for energy, which restricts the entry of pyruvate into the tricarboxylic acid (TCA) cycle to undergo oxidative phosphorylation, and thus promotes the malignant biological behavior of gastric cancer cells [4, 5]. On the other hand, PDK blocks pyruvate from entering the TCA by inhibiting PDH activity, thereby enhancing anaerobic glycolysis and lactate production. Glycolysis leads to the accumulation of acidic metabolic byproducts, such as lactate, which creates an acidic tumor microenvironment. This acidic environment has been demonstrated to reduce the effectiveness of radiotherapy. The pentose phosphate pathway (PPP), a branch of glycolysis, generates significant amounts of nicotinamide adenine dinucleotide phosphate (NADPH). NADPH is crucial for maintaining intracellular levels of reduced glutathione (GSH) and scavenging ROS. High NADPH levels can help tumor cells resist the oxidative stress induced by radiotherapy, thereby contributing to resistance. Sustained activation of PDK can influence various pro-survival and anti-apoptotic signaling pathways, such as the phosphoinositide 3-kinase/protein kinase B/mammalian target of rapamycin (PI3K/Akt/mTOR) and hypoxia-inducible factor 1- α (HIF-1 α) pathways, which are closely associated with radiotherapy resistance. Ionizing radiation produces damaging effects on cells, including direct damage to cellular DNA and indirect damage mediated by free radicals and ROS. Pyruvate is a product of glycolysis and is located at the “crossroads” of glycolysis and mitochondrial respiration. Studies have shown that pyruvate is a “scavenger” of ROS and can enhance the antioxidant response of solid tumors during radiotherapy [6]. Glucose metabolism and metabolic intermediates in tumor cells are closely related to radiotherapy resistance and can predict the response of individual tumors to radiation therapy [7]. Glycolysis also enhances radioresistance by promoting DNA damage repair, which provides a theoretical rationale for the use of glycolysis-inhibiting drugs to increase sensitivity to radiotherapy [8]. Enhanced glycolysis in solid tumors significantly increases the secretion of lactic acid, which has antioxidant capacity, and its concentration is positively correlated with radiotherapy resistance.

Intervention targeting PDK can disrupt the dependence of tumor cells on glycolysis, inducing energy crisis and even cell death. PDK sits at the crucial interface between the glycolytic pathway and the tricarboxylic acid cycle, functioning as a “gating enzyme” in tumor metabolic reprogramming. Direct intervention at this key node often results in more significant disruptions in energy metabolism compared to inhibiting downstream or bypass metabolic pathways. Compared to glycolytic enzymes such as GLUT1 and LDH-A, the expression and activity of PDK in normal tissues exhibit a certain degree of plasticity. Literature reports indicate that PDK inhibitors within a reasonable dosage range are more easily tolerated by patients and the metabolic impact on normal cells is often more controllable. DCA is a pyruvate mimetic that binds to and inhibits the activity of PDK, which can alter tumor metabolism by activating the activity of mitochondria, forcing the tumor cells to shift from glycolysis to oxidative phosphorylation, which makes tumor cells more susceptible to radiotherapy-induced damage [9]. Tumor cells in an oxidative phosphorylation state are more susceptible to DNA damage induced by radiotherapy. DCA has shown antitumor activity in preclinical models of a variety of cancers and has been subjected to a number of preliminary clinical trials showing some safety. Research has shown that DCA enhances the radiosensitivity of medulloblastoma, potentially through inhibiting glycolysis, increasing ROS production, and reducing cancer stem-like characteristics [10]. Furthermore, the combination of DCA with radiation improves survival rates in glioblastoma mouse models, with mechanisms involving cell cycle arrest, increased oxidative stress, and DNA damage [11]. DCA has been found to augment the antitumor effect of hypoxic cytotoxins in solid tumors [12]. DCA has been proven to enhance radiosensitivity in breast cancer [13], colon cancer [14], prostate cancer [15], esophageal cancer [16], and glioblastoma [11]. Currently, there is a lack of sufficient experimental evidence to support the relationship between PDK activity and the efficacy of radiotherapy in gastric cancer, as well as the potential radiosensitizing effect and molecular mechanism of PDK inhibitor DCA in gastric cancer radiotherapy, which warrants further investigation. In addition, DCA is a relatively readily available and low-cost compound, facilitating laboratory studies and potential clinical translation. Therefore, the present study was designed to elucidate the role and mechanism of DCA, a PDK inhibitor, on the progression of gastric cancer cells and sensitization by radiotherapy.

2 Materials and methods

2.1 Immunohistochemical staining analysis

Gastric cancer prognostic tissue microarrays (ZL-STC1601) were purchased from Vio Biotech (Shanghai, China). The microarrays were stained with immunohistochemistry (IHC) staining kit (Bios Biological Technology Company, China) and anti-PDK antibody (Wuhan Sanying Biotechnology Co., Ltd., Wuhan, China). The number of positives and the intensity of staining in each section were converted into corresponding values by Histochemistry score to achieve semi-quantitative

staining of tissues. (H-SCORE = $\sum(p_i \times i)$) = (percentage of weak intensity $\times 1$) + (percentage of moderate intensity $\times 2$) + (percentage of strong intensity $\times 3$), where p_i represents the positive signal pixel area/cell number percentage; i represents coloring intensity; H-score is the data between 0 and 300, the larger the data indicates the stronger the integrated positive intensity). Statistical analysis and survival curves were plotted using Graphpad Pism 9.5 software.

2.2 Cell lines and cell culture

MKN-45 and AGS were purchased from Procell Wuhan, and GES-1 and HGC-27 cells were provided free of charge by the laboratory of Gansu Provincial People's Hospital. All cell lines were characterized by short tandem repeat (STR) analysis and detected for mycoplasma contamination. The cells were cultured in RPMI-1640 medium supplemented with 10% fetal bovine serum (FBS) and 1% penicillin/streptomycin (P/S) and placed in an incubator at 37°C and 5% CO₂. Cell culture reagents were purchased from Biological Industrise, Israel.

2.3 Real-time fluorescence quantitative PCR (RT-qPCR) assay

Total RNA from the cells was extracted using M5 Universal RNA MiNi Kit (Mei5bio, Beijing, China). reverse transcription was performed using M5 Sprint qPCR RT kit. Real-time qPCR was performed on a LightCycler Nano real-time fluorescent quantitative PCR instrument using M5 HiPer SYBR Premix EsTaq (Mei5bio, Beijing, China). gAPDH was used as an internal control for mRNA. Relative RNA expression levels were calculated as $2^{-\Delta\Delta Ct}$. Relevant primer sequences and reaction systems are listed in Additional file Tables 1–5.

2.4 CCK8 cell proliferation assay

DCA is a specific inhibitor of PDK and inhibits PDK activity. Gastric cancer cells MKN-45, AGS were inoculated into 96-well plates at about 8000 cells per well, and the complete medium was added and placed in the incubator. After 24 h of incubation, the waste liquid of each well was aspirated and discarded. DCA was prepared with RPMI 1640 medium at concentrations of 0, 20, 40, 60, 80, and 100 mM, and subsequently added to each group, with six parallel replicate well groups in each group. CCK8 reagent (APExBIO, United States of America) was added 10 μ L per well at 24 h, 48 h and 72 h, respectively, under the condition of light protection. 96-well plates were placed in an incubator at 37 °C, and the absorbance values were measured using an enzyme marker after incubation for 1 h. IC50 was calculated and plotted by GraphPad Prism 9.5 software.

2.5 Cell proliferation assay

Control and ADC-treated cells (MKN-45, AGS) were inoculated into 6-well plates at approximately 10⁴ cells per well, and 2X of EdU working solution prepared according to the EdU assay kit (Beyotime, Shanghai, China) was added to the well plates with an equal volume of culture medium to incubate the cells for 2 h. After EdU labeling of the cells was completed, the culture medium was removed, and the cells were incubated for 2 h by adding 1 ml of 4% paraformaldehyde (Beyotime, Shanghai, China) for 15 min at room temperature for fixation. The treated groups of cells were observed under a fluorescence microscope (Olympus BX51, Japan) for cell proliferation. The percentage of Edu-positive cells and the average fluorescence intensity were calculated using Image J software (NIH, USA).

2.6 Migration tests

The two groups of cells were inoculated separately at approximately 10⁵ cells per well in Falcon chambers of 8.0 μ m pore size with serum-free medium (Transwell, Corning Life Sciences, Acton, MA, USA). 700 μ L of medium containing 10% FBS was added to the lower chamber, and 200 μ L of complete medium was added to the upper chamber. The chambers were then placed in an incubator at 37 °C and 5% CO₂ for 24 h. Cells remaining in the upper chamber were then carefully removed with a cotton swab. The Transwell membrane of the lower chamber was fixed with 4% paraformaldehyde for 30 min and stained with 0.1% crystal violet for 15 min, and after washing to remove the crystal violet, photographs were taken under a microscope, and the migration level of cells in each group was evaluated using ImageJ software.

2.7 Flow cytometry test

The two groups of cells were inoculated into 6-well plates at about 2×10^5 cells per well, and after 24 h of culture, the cells in each group were incubated at room temperature and protected from light using the Cell Cycle and Apoptosis Analysis Kit (Elabscience, Wuhan, China), and the processed cells were up-examined using a FACS Calibur flow cytometer. The relative proportion of apoptotic cells was detected by FlowJo 10.8.1 software; the percentage of cells in each phase was detected by ModFit LT 5.0 software.

2.8 Lactic acid testing

The two groups of cells were inoculated into 24-well plates with 2×10^3 cells per well and cultured with complete medium for 24 h. After 24 h, the cells were irradiated under a 6 MV medical electron linear accelerator (Siemens, German) at a dose of 4 Gy; after 24 h, they were further processed according to the instructions of the Lactic Acid Content Detection Kit (Solarbio, Beijing, China); finally, the processed cells were partitioned into 96-well plates and placed on the enzyme labeling instrument. Finally, the treated cells were divided into 96-well plates and placed on an enzyme labeler, and the absorbance value of each well was measured at 530 nm and calculated and plotted using GraphPad Prism 9.5 software.

2.9 Clone formation experiments

In order to study the sensitivity of gastric cancer cells to radiation, two groups of cells were inoculated into 6-well plates at 200, 400, 600, 800, and 1000 cells per well, respectively, and added with complete medium and placed in the incubator. After 24 h of incubation, the cells containing 400, 600, 800, and 1000 were placed in a 6 MV medical electron linear accelerator (Siemens, German) for radiation at doses of 2 Gy, 4 Gy, 6 Gy, and 8 Gy, respectively. Subsequently, the supernatant was discarded, and the culture was replaced with fresh complete medium; the medium was changed every 2–3 days, and the growth status of the cells was observed until visible colonies were observed. After washing and fixation, the colonies were stained with crystal violet. Colonies containing more than 50 cells were counted and the results were analyzed with ImageJ software to generate a radiobiological parameter table.

2.10 ROS testing

The two groups of cells were inoculated into 6-well plates at 10^4 cells per well and cultured with the addition of complete medium. After 24 h of incubation, the cells were irradiated with 6 MV medical electron linear accelerator (Siemens, German) at a dose of 4 Gy after replacing the fresh complete medium. After 48 h of incubation, DCFH-DA (Beyotime, China) was diluted with RPMI 1640 medium at a dilution ratio of 1000:1 to make the final concentration of 10 $\mu\text{mol/L}$; the waste liquid was discarded, and about 1.5 ml of diluted DCFH-DA was added to each well and incubated for 20–30 min in a cell culture incubator at 37 °C. Incubate the cells in cell culture chamber for 20–30 min; Wash the cells with RPMI 1640 medium three times to fully remove the fluorescent probe DCFH-DA that did not enter into the cells; Observe using inverted fluorescence microscope and take photos for recording.

Gastric cancer cells MKN-45 and AGS were seeded into a 24-well plate at 8,000 cells per well in complete medium. After 24 h of incubation, the medium was replaced with RPMI 1640 containing DCA at concentrations of 0, 20, and 40 mM (with three replicates per concentration). Following another 24 h of culture, the cells were irradiated with a 6 MV medical linear accelerator at a dose of 4 Gy. After 48 h post-irradiation, DCFH-DA was diluted in RPMI 1640 to a final concentration of 10 $\mu\text{mol/L}$ and added to the cells after removing the old medium and washing with PBS. The cells were then trypsinized, collected, and centrifuged twice at 1500 rpm for 5 min each time with PBS resuspension. After adjusting the cell concentration to ensure consistency among groups, approximately 0.8 mL of diluted DCFH-DA was added to each group. The cells were incubated for 20–30 min at 37 °C, washed three times with RPMI 1640 to remove any unincorporated fluorescent probe, and then transferred to a 96-well plate under dark conditions. Fluorescence intensity was measured using a fluorospectrometer with settings at an excitation wavelength of 488 nm and an emission wavelength of 525 nm.

2.11 γ -H2AX assay

The two groups of cells were inoculated into 6-well plates at 10^5 cells per well and cultured with the addition of complete medium. After 24 h of incubation, the cells were placed in 6 MV medical electron linear accelerator (Siemens, German) irradiation at a dose of 4 Gy after replacing the fresh complete medium. After 48 h of incubation, the GC cells were lysed in RIPA lysate (Dr. Wuhan). The total protein concentration of each group was determined by BCA protein assay kit (Dr. Wuhan). Aliquots of protein samples were separated by SDS-PAGE SWE (Rapid High Resolution Electrophoresis Buffer, Sevier, Wuhan) and transferred onto PVDF membranes (Merck Millipore, Ireland). After sealing with skimmed milk, primary and secondary antibodies were performed for target protein expression. The final exposure was used to obtain the γ -H2AX (CST, USA) expression map of each group, and β -Tubulin was used as an internal reference.

2.12 Statistical analysis

All data are expressed as mean \pm standard deviation. Data were analyzed using SPSS 25.0 (SPSS, USA) and GraphPad Prism 9.5 (GraphPad, USA). Kaplan–Meier curve analysis was used to assess survival, and t-tests, ANOVA, or chi-square tests were used to assess differences between groups. A P-value of < 0.05 was considered statistically significant, and significance is indicated as follows: ns, not significant, $P > 0.05$; *, $P < 0.05$; **, $P < 0.01$; ***, $P < 0.001$; ****, $P < 0.0001$.

3 Result

3.1 High expression of PDK in gastric cancer tissues correlates with prognosis

To investigate the expression of PDK, we performed immunohistochemical analysis in 60 paired gastric cancer and paracancerous tissue specimens. IHC-stained sections of gastric cancer and paracancerous tissues showed that PDK1 was significantly overexpressed in cancerous tissues (Fig. 1A, B). We also found that PDK1 expression correlated with patient prognosis, and GC patients with high PDK1 expression levels had lower survival rates (Fig. 1C). RT-PCR analysis showed that PDK1 mRNA levels were significantly up-regulated in gastric carcinoma MKN-45 and AGS cell lines compared with normal gastric epithelial cell lines (GES-1) (Fig. 1D).

To evaluate the biotoxicity of the PDK inhibitor DCA on gastric cancer cells, a concentration gradient of DCA was set at 0 mM, 20 mM, 40 mM, 60 mM, 80 mM, and 100 mM, which acted on AGS and MKN-45 cells, respectively, and the cellular activities were determined at 24 h, 48 h, and 72 h, respectively. The results showed that the cell proliferation activity gradually decreased with increasing DCA dose and time, and DCA inhibited the proliferation of gastric cancer cells in a dose-dependent and time-dependent manner (Fig. 1E, F, Tables 6–7 in Additional file). Statistical analysis using GraphPad Prism 9.5 yielded an IC₅₀ of 47.94 mM and 44.19 mM for DCA inhibition of AGS and MKN-45 cells, respectively. In addition, the IC₂₀ of DCA inhibition of AGS and MKN-45 cells was 22.21 mM and 17.56 mM, respectively. Therefore, in this experiment, the use of a concentration of 40 mM of DCA with AGS and MKN-45 gastric cancer cells for subsequent studies.

3.2 Effects of DCA on the biological behavior of gastric cancer cells

To explore the effect of PDK inhibitor DCA on the malignant progression of GC cells, we performed EdU assays, which showed that DCA reduced the proliferation of GC cells AGS and MKN-45 (Fig. 2A). Transwell migration assay showed that DCA decreased the migration of GC cells AGS and MKN-45 (Fig. 2B). The effects of the PDK inhibitor DCA on cell cycle and apoptosis were analyzed by flow cytometry. The results showed that inhibition of PDK in AGS and MKN-45 cells increased the number of cells in the G1 phase compared with the respective negative controls (Fig. 2C). Meanwhile, inhibition of PDK enhanced the apoptosis rate of GC cells MKN-45 and AGS cells (Fig. 2D). These results clearly indicated that high expression of PDK promoted the malignant biological behavior of GC cells.

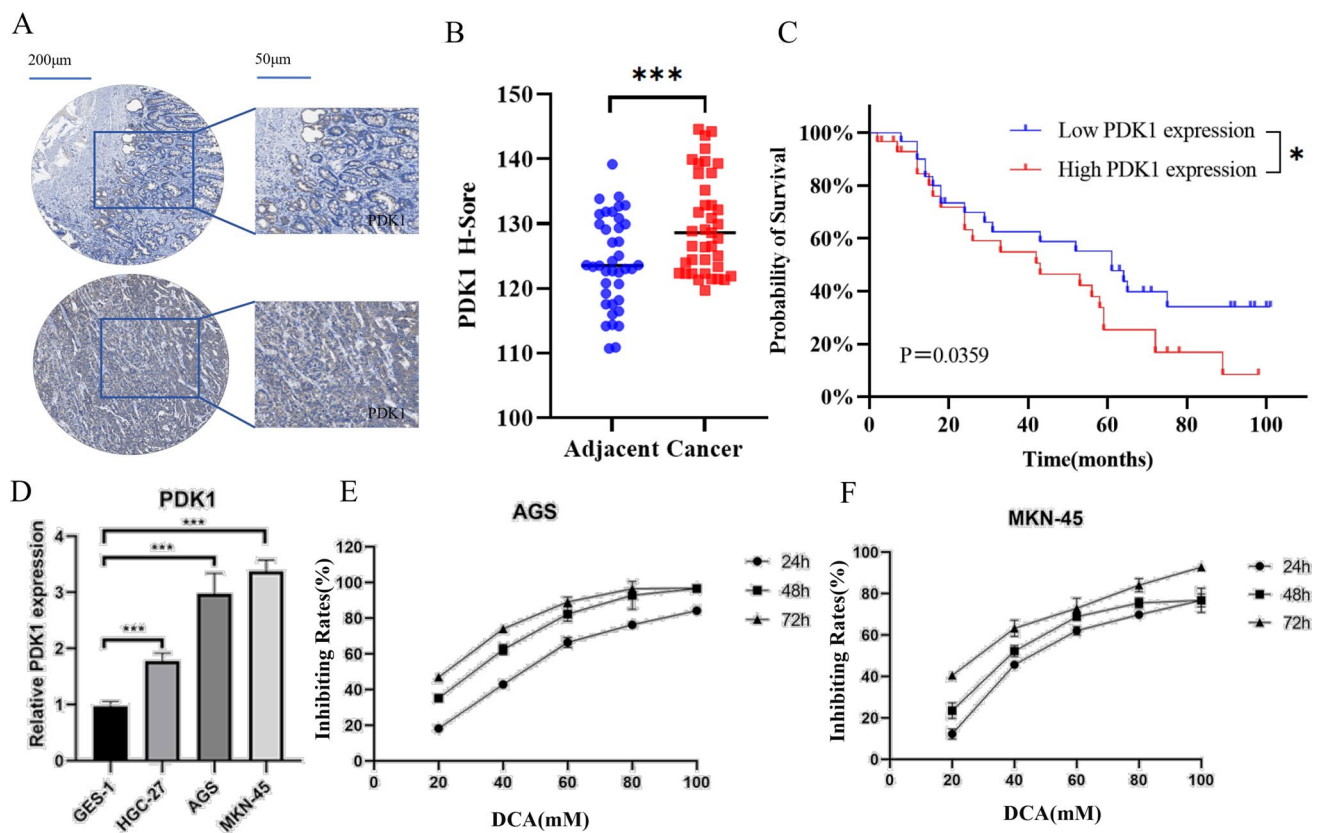


Fig. 1 Expression of PDK1 in gastric cancer tissues and cells. **A** IHC plots of PDK1 in paracancerous and cancerous tissues of gastric cancer. **B** The IHC staining intensity was converted to the corresponding H-Score value, and the larger value indicated the stronger intensity of the integrated positive staining. **C** Survival curves of GC patients with high/low expression of PDK1 were plotted using the Kaplan–Meier and Mantel–Cox tests. **D** RT-PCR was performed to detect PDK1 expression in the gastric cancer cells and gastric mucosal epithelial cells. **E, F.** CKK8 was used to detect the inhibitory effect of DCA on the proliferation of gastric cancer cells. * $P < 0.05$, ** $P < 0.01$, *** $P < 0.001$

3.3 DCA affects PDK-mediated glycolysis

The PDK1 co-expressed genes are shown in Fig. 3A, in which CDIPT and UBE2J1 showed strong correlation with PDK1 expression ($r = -4.520E-01$, $4.571E-01$, $P = 2.771E-22$, $8.217E-19$, respectively). As shown in Fig. 3C, the GO biological processes of PDK1 co-expressed genes were mainly enriched in ribonucleic acid localization, ncRNA processing, cell cycle checkpoints, double-stranded DNA break repair, etc.; GO cellular components were mainly enriched in ribosomes and DNA damage sites, etc.; GO molecular functions were enriched in deconjugating enzyme activities, catalytic activities, etc.; and KEGG pathway analyses showed that these genes were mainly associated with RNA transport, aminoacyl-tRNA biosynthesis, cell cycle, homologous recombination, RNA degradation and so on. Taken together, PDK1 expression may play an important role in gastric cancer development by regulating nucleotide formation, cell cycle regulation and DNA double-strand break repair. In the STRING database, the target protein PDK1 was searched and the protein interaction network was shown in Fig. 3B. In the network, pyruvate dehydrogenase kinase isozyme 2(PDK2), pyruvate dehydrogenase kinase isozyme 3(PDK3), pyruvate dehydrogenase X component(PDHX), pyruvate dehydrogenase A1(PDHA1), pyruvate dehydrogenase A2(PDHA2), pyruvate dehydrogenase B(PDHB), dihydrolipoamide dehydrogenase(DLD), lactate dehydrogenase A(LDHA) and hypoxia-inducible factor 1α(HIF1A) are closely related to PDK1.

Our group has been eager to explore whether metabolic alterations in gastric cancer affect radiotherapy resistance, so we investigated the effect of the PDK inhibitor DCA on glycolysis in gastric cancer. AGS and MKN-45 cells were treated with 20 and 40 mM DCA, respectively, and the results showed that DCA inhibited lactate production, and the difference between the groups was statistically significant ($P < 0.05$). However, there was no significant difference between the interventions in the radiation alone and DCA alone groups (Fig. 3D). The reduction of lactate

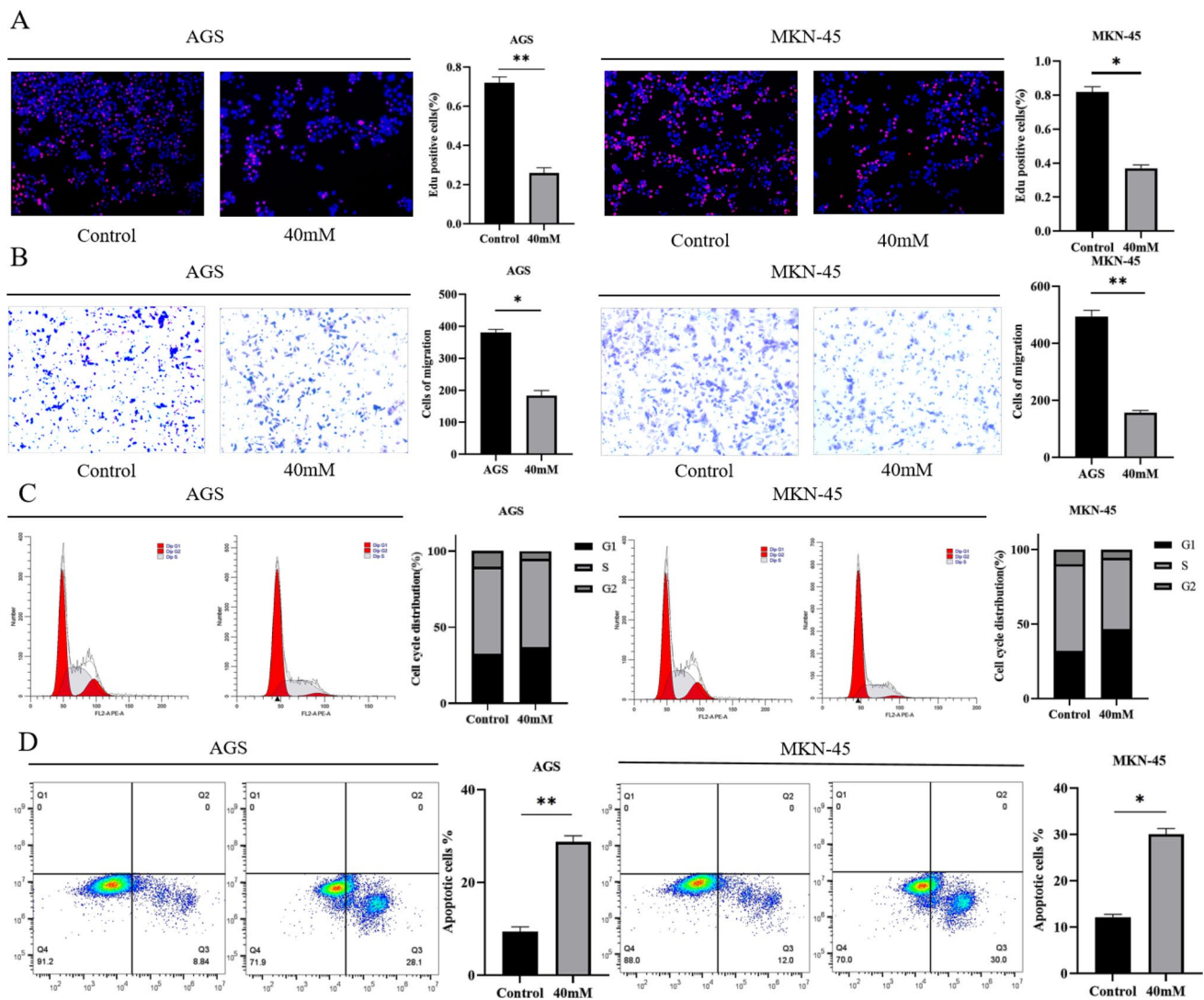


Fig. 2 Effect of DCA on biological behavior of gastric cancer cells. **A** Cell proliferation detection by Edu assay (10x). **B** Cell migration exploration by Transwell assay (10x). **C** Proportion of cells in G1, S and G2 phases was detected by FACS analysis. **D** Apoptosis rate of gastric cancer cells after ADC treatment was detected by FACS analysis. * $P < 0.05$, ** $P < 0.01$, *** $P < 0.001$

production in the 4 Gy combined with 20 mM DCA group compared with the lactate content in the 4 Gy radiation treatment alone group was considered to be related to the inhibition of lactate production by DCA. Therefore, PDK inhibitor DCA inhibited lactate production and radiation did not affect lactate production, which was consistent with the group's pre-prediction. The above experiments further confirmed that DCA could inhibit glucose metabolism in gastric cancer cells, and this regulatory mechanism was not affected by radiation.

3.4 Effect of DCA on colony formation in irradiated gastric cancer cells

In order to test whether the PDK inhibitor DCA has a radiosensitizing effect on gastric cancer cells AGS and MKN-45, 20 mM DCA was selected to intervene in gastric cancer cells AGS and MKN-45 according to the concentrations of IC₂₀ (22.21 mM) for AGS and IC₂₀ (17.56 mM) for MKN-45. Cell clone formation assay was used, which was analyzed by the multi-targeted single-hit model ($SF = 1 - (1 - \exp(-D/D_0))^N$) was analyzed, where $D_q = D_0 \log_e(N)$. The mean lethal dose D_0 , the shoulder region of the survival curve D_q and the sensitization ratio (SER) were calculated by GraphPad Prism 9.5 software. Survival fraction at 2 Gy (SF₂) is an indicator of cellular radiosensitivity to radiation [17]. SF₂ ranges from 0 to 1, with lower SF₂ indicating higher radiosensitivity. We fitted survival curves and tabulated radiobiological parameters using a multi-target single-hit model based on the results of cell clone formation by DCA inhibition of AGS, MKN-45 (Fig. 4A,

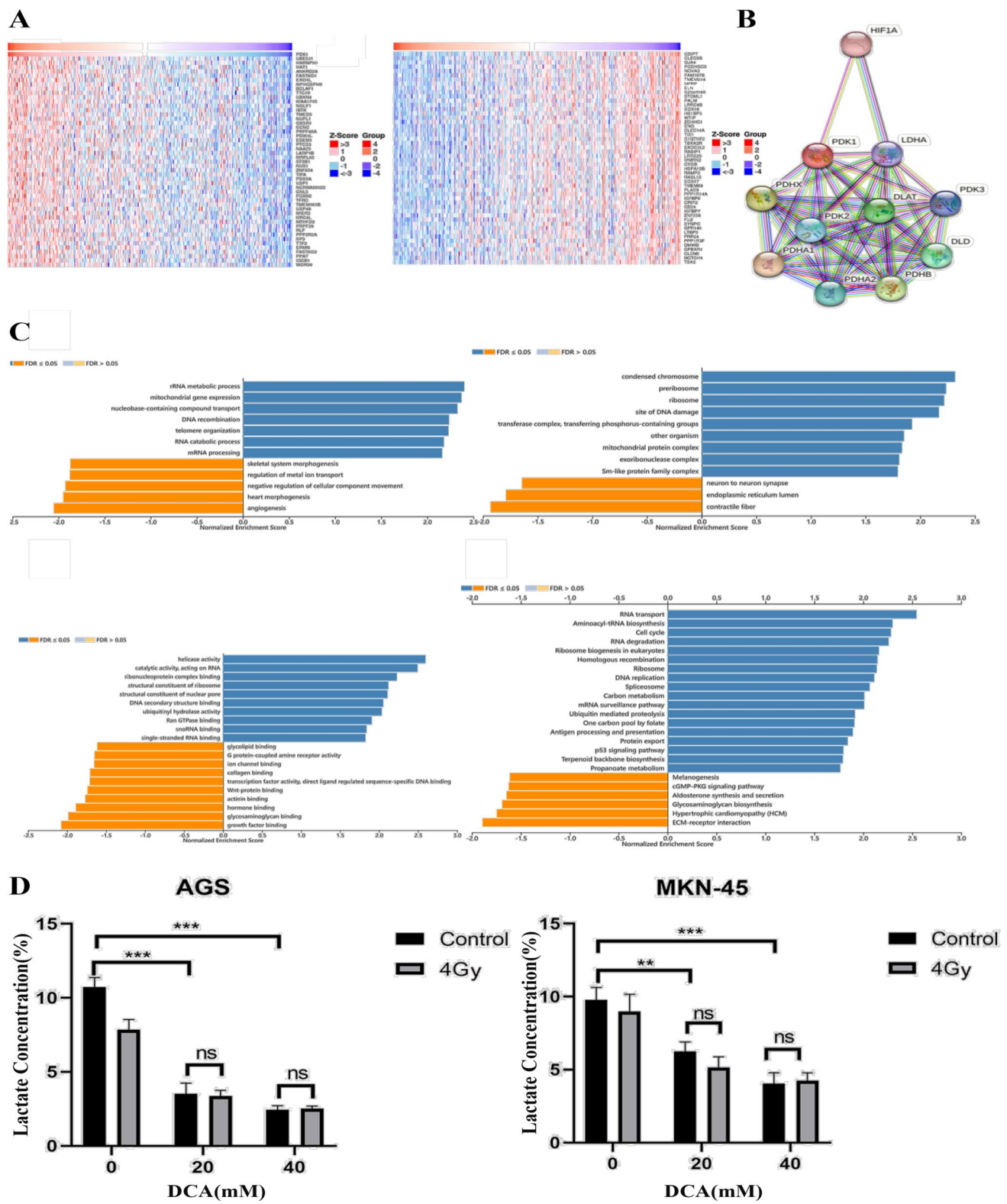


Fig. 3 Effect of DCA on glucose metabolism in gastric cancer cells. **A** PDK1 enrichment analysis of volcanoes and highly closely related genes; **B** Protein interaction network analysis of PDK1 showed that PDK1 was associated with numerous glycolytic enzymes. **C** PDK1 co-expression gene enrichment analysis showed that gastric cancer PDK1 was associated with processes such as nucleotide metabolism and DNA repair (GO bioprocesses, GO cellular components, GO molecular functions, and KEGG functional analysis). **D** Effects of DCA and radiation on lactate content of gastric cancer cells. * $P < 0.05$, ** $P < 0.01$, *** $P < 0.001$, ns for $P > 0.05$

B, C). Compared with the cells in the AGS alone radiation group, the cells in the radiation combined with 20 mM DCA group showed reduced clone formation ability and a significant decrease in cell proliferation with an SER of 1.38. In the MKN-45 cells, the cells in both the radiation alone group and the radiation combined with 20 mM DCA group showed a reduction in the clone formation ability and a decrease in the cell proliferation with an SER of 1.43. The results of the above experiments indicated that the PDK inhibitor DCA enhanced the radiosensitivity of gastric cancer cells and had a sensitizing effect of radiotherapy.

3.5 Effect of DCA on gamma-H2AX production in irradiated gastric cancer cells

DNA double-strand breaks are an important form of cellular damage by radiation, and DNA double-strand breaks induce the formation of γ -H2AX, which is one of the markers of DNA double-strand breaks [18]. In this study, protein immunoblotting was utilized to measure the protein levels of γ -H2AX after radiation (4 Gy), DCA (40 mM) intervention and combined intervention. Figure 4D, E, In AGS and MKN-45 cells, a statistically significant increase in γ -H2AX abundance was observed after radiation alone and radiation combined with DCA intervention ($P < 0.001$). Based on these results, the combined radiation and DCA intervention significantly increased γ -H2AX production and DNA double-strand damage, confirming that DCA has a radiosensitizing effect.

3.6 Effects of DCA on ROS production in irradiated gastric cancer cells

Since DCA increases oxidative stress by prompting pyruvate to enter the mitochondria and increases the activity of the electron transport chain, which results in the generation of more ROS, this may be the basis for the sensitization of DCA radiotherapy. In this study, we used the PDK inhibitor DCA combined with radiation to intervene in gastric cancer cells, and then the fluorescence intensity of ROS was measured by fluorescence enzyme labeling, which showed that the generation of ROS was significantly increased in the DCA combined with radiation group compared with the other groups ($P < 0.001$, Fig. 4F). Subsequently, using a fluorescence microscope, intracellular ROS levels were observed after the addition of the fluorescent probe DCFH-DA to the cells in each group. 40 mM DCA combined with 4 Gy radiation revealed that the intensity of green fluorescence in AGS and MKN-45 cells was significantly stronger than that in the blank control group (Fig. 4G). The above experimental results indicated that the combined intervention of radiation and DCA elevated the ROS level in gastric cancer cells, and DCA increased ROS generation by increasing oxidative phosphorylation.

4 Discussion

Previous studies have shown that PDK1 is highly expressed in many cancers, such as head and neck squamous carcinoma, gastric carcinoma, intestinal carcinoma, ovarian carcinoma, and breast carcinoma [19]. In this experiment, we showed that PDK1 expression was increased in gastric cancer tissues and cells by pathological tissue microarray and fluorescence quantitative PCR analysis, and it was consistent with the results of bioinformatics analysis mentioned above. In addition, immunohistochemistry of gastric cancer tissues obtained from patients who underwent radical resection revealed that high PDK-1 expression was one of the biomarkers of poor prognosis for patients treated with 5-fluorouracil [20]. Our survival analysis also reconfirmed that high PDK-1 expression may be a biomarker of poor prognosis in gastric cancer patients.

DCA is a pyruvate mimetic that competes with pyruvate for the binding of PDK. DCA was initially used in the clinical treatment of lactic acidosis [21]. Inhibition of PDK by DCA facilitates the entry of pyruvate into the tricarboxylic acid cycle and shifts metabolism from glycolysis to oxidative phosphorylation [22]. This metabolic “normalization” increased mitochondrial respiration and reactive oxygen species production, inhibited the proliferation of ovarian cancer cells [23] and hepatocellular carcinoma cells [24], and induced apoptosis. In the present study, we showed by CCK8 assay that the PDK inhibitor DCA inhibited the proliferation of GC cells in a dose- and time-dependent manner. It was shown by Transwell assay that PDK inhibitor DCA inhibited the migration of gastric cancer cells. It was shown by flow cytometry experiments that PDK inhibitor DCA increased the number of GC cells in G1 phase and simultaneously increased the apoptosis rate of GC cells. Our results suggest that high expression of PDK promotes the malignant biological behavior of GC cells.

PDK1 was associated with DNA double-strand break repair by enrichment analysis of PDK1. In this study, we explored the effects of ionizing radiation synergizing PDK on in vitro cultured GC cells. Ionizing radiation produces lethal effects on cells mainly through ionization of cellular biomolecules. Ionizing radiation effects include direct damage to cellular

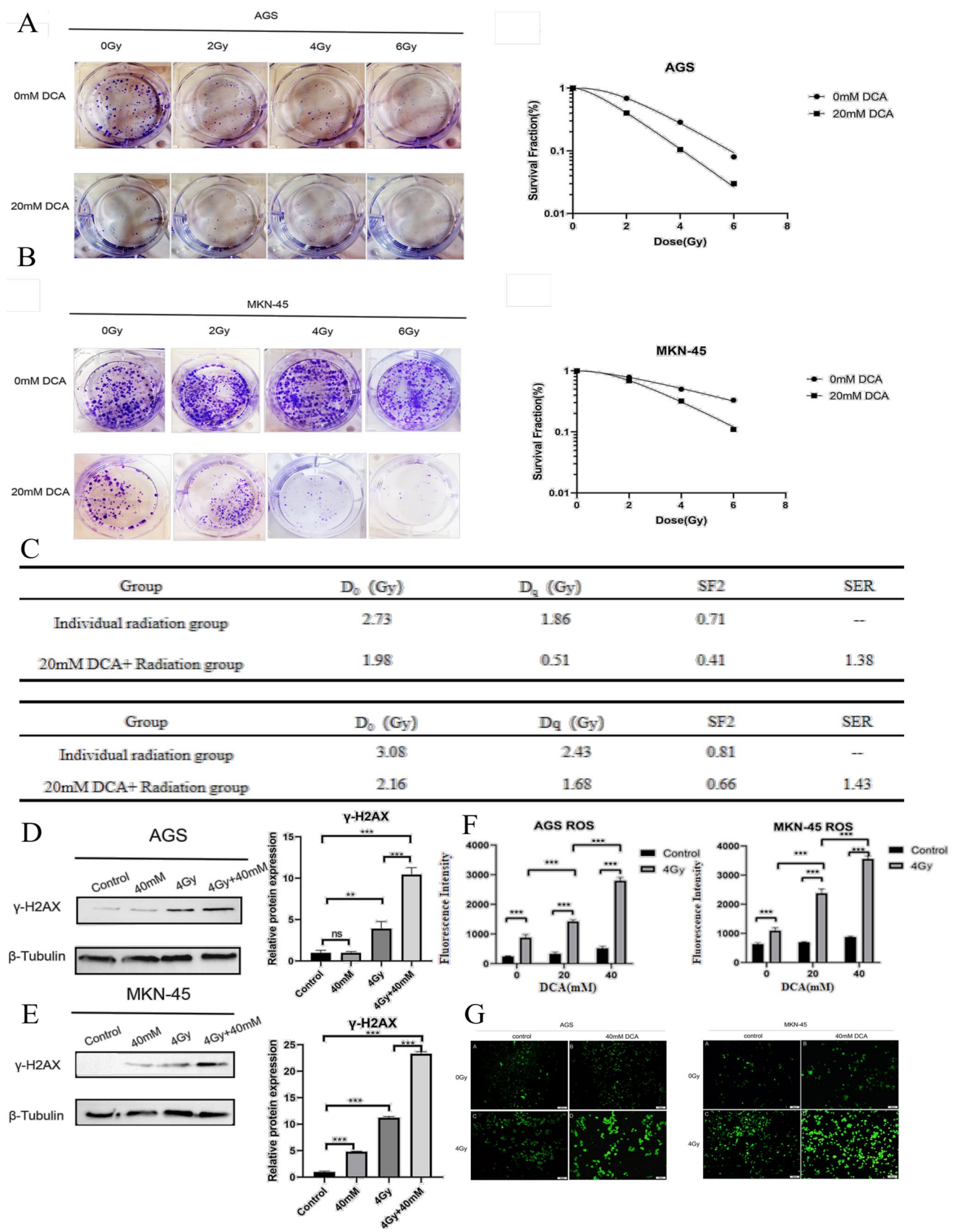
Fig. 4 Effect of DCA on the sensitivity of gastric cancer cells to radiotherapy. **A, B** DCA co-radiation intervention to explore the survival of gastric cancer cells and fit the cell dose survival curves; **C** Inhibition of PDK expression to generate the radiobiological parameter table of AGS, MKN-45 in gastric cancer cells. **D, E** The effect of DCA co-radiation on the production of γ -H2AX in gastric cancer cells. **F** Fluorescence zymography to detect the effect of DCA co-radiation on the ROS content of gastric cancer cells. **G** Fluorescent probe method to observe the effect of DCA co-radiation on ROS content of gastric cancer cells (10x). * $P < 0.05$, ** $P < 0.01$, *** $P < 0.001$, ns for $P > 0.05$

DNA, indirect damage by radiolysis of water molecules leading to free radicals and ROS production, and oxidative stress by secondary damage to subcellular structures and biomolecules [25]. Ionizing radiation can lead to DNA double-strand breaks and consequently γ -H2AX accumulates at the site of DNA double-strand breaks [26]. Therefore, γ -H2AX can be used as a biological dosage tool for radiation sensitivity. As shown by cell clone formation assay and protein blotting assay, the PDK inhibitor DCA combined with radiation intervention in gastric cancer cells significantly inhibited cell proliferation and promoted the formation of γ -H2AX, indicating that DCA was able to produce radiosensitization.

A large number of previous studies have confirmed that glucose is aerobically glycolysed in tumor cells to produce lactate. DCA inhibits glycolysis by activating the mitochondrial pyruvate dehydrogenase complex, while reducing lactate production [27]. Measurement of lactate concentration in primary tumors can be used as a basis for metabolic classification, and targeting lactate metabolism may also improve cancer prognosis and treatment [28]. In this study, we measured the concentration of lactate in the supernatant of gastric cancer cells to investigate the relationship between glucose metabolism and radiation effects. The results showed that the PDK inhibitor DCA inhibited lactate production in gastric cancer cells, while the changes in lactate production were not significant after radiation intervention in gastric cancer cells. We have noted that radiation exposure typically upregulates LDHA via HIF-1 and enhances lactate production. However, significant upregulation of LDHA in the irradiated group was not observed in the data from this study, which may be related to the following factors: 1. Differences in experimental time windows: The detection time point post-radiation (24 h) in this study may be later than the typical peak of HIF-1 activation (usually 4–12 h), leading to feedback inhibition; 2. Cell type specificity: The primary gastric cancer cells used in this experiment exhibited low expression levels of HIF-1 under normoxic conditions, which may also result in blunted HIF-1 responsiveness to radiation due to metabolic reprogramming and other factors. Previous studies have suggested that higher lactate accumulation in malignant tumors may predict radiation resistance [29]. However, it has also been shown that there is no correlation between the rate of lactate production in single cells in vitro and lactate concentration in vivo. This may be due to the different rates of lactate production in vivo and in vitro [30]. In addition, it is possible that the tumor microenvironment may also affect the in vivo lactate concentration [30].

Ionizing radiation can not only damage DNA directly, but also induce DNA damage indirectly by increasing ROS production [31]. Ionizing radiation can increase ROS production by inducing extracellular water radiolysis or mitochondrial damage [32]. Previous studies have shown that the PDK inhibitor DCA reduces tumor cell proliferation and promotes sensitization of breast cancer cells to radiotherapy by inducing ROS [4]. DCA enhances mitochondrial oxidative metabolism by inhibiting PDK, theoretically indirectly inducing DNA damage through ROS. However, a significant increase in γ -H2AX was not observed in this study, which may be related to the following factors: 1. The 24-h DCA treatment may not have been sufficient to accumulate adequate ROS, and the oxidative stress induced by DCA may have been effectively buffered by the cellular antioxidant system; 2. It may be due to complex interactions among other signaling pathways activated or inhibited by DCA. In the present study, it was found that the combination of DCA and radiation was able to significantly increase ROS levels. Therefore, the group speculated to consider that the PDK inhibitor DCA may promote gastric cancer cell sensitization to radiotherapy by increasing ROS production.

The tumor microenvironment (TME) is a highly complex and dynamic ecosystem composed of immune cells, stromal cells, and the extracellular matrix (ECM), which interact intricately to regulate cancer progression and the response to therapy. Immune cells, such as tumor-associated macrophages (TAMs) and T cells, can either promote or inhibit tumor growth. Stromal cells, including cancer-associated fibroblasts (CAFs), secrete various growth factors and cytokines that facilitate tumor progression. Additionally, the ECM provides structural support for tumor cell migration and invasion. Recent studies have underscored the critical role of the TME in tumor biology and therapeutic responsiveness. For example, research by Lui et al. has demonstrated promising strategies to reverse T-cell exhaustion and enhance antitumor immunity in non-small cell lung cancer (NSCLC) [33]. However, the immunosuppressive nature of the TME—characterized by elevated levels of inhibitory cytokines, immunosuppressive immune cell subsets, and upregulated immune checkpoint receptors—contributes significantly to T-cell dysfunction, thereby impairing effective antitumor responses. Moreover, a study by Xu et al. identified fibronectin type III domain-containing protein 4 (FNDC4) as a secreted protein with extracellular structural domains functionally resembling components of the ECM [34]. FNDC4 has emerged as a potential prognostic



biomarker and predictor of immunotherapy response in lung adenocarcinoma. PDKs, particularly through their pivotal role in metabolic reprogramming, have been shown to enhance the reliance of tumor cells on glycolysis. This metabolic shift not only supports tumor cell survival under hypoxic conditions typically found in the TME but also modulates the functional state of immune cells within the microenvironment. For instance, elevated expression of PDKs in TAMs drives their polarization toward the immunosuppressive M2 phenotype, thereby promoting immune evasion within the TME. Additionally, accumulating evidence suggests that pharmacological inhibition of PDKs can reverse T-cell exhaustion, restore cytotoxic function, and potentially improve the efficacy of immune checkpoint inhibitors (ICIs). Therefore, PDKs are not only key regulators of tumor metabolic reprogramming but are increasingly recognized as central modulators of immune activity within the TME. Elucidating the mechanistic roles of PDKs in shaping the immune landscape of the TME may offer novel insights and therapeutic opportunities for the development of combined metabolic-immunologic cancer therapies.

Several difficulties and challenges remain for the future clinical translation of DCA. At pharmacologically achievable doses, the PDK inhibitor DCA acts synergistically with antitumor agents such as 5-fluorouracil, cisplatin, and sorafenib [35–37]. Inhibiting glycolytic energy sources and forcing tumor cells to use mitochondrial sources induces more ROS generation and activates cell death signaling. However, DCA binds weakly to PDK due to the fact that some tumor cells silence the proteins that transport DCA through epigenetic mechanisms, so DCA requires higher doses to exert its pharmacological effects [38]. In addition, prolonged use of DCA can cause hepatic injury through inhibition of glutathione transferase and oxidative damage to nerves, leading to peripheral neuropathy [39]. Since this study was limited to raw letter analysis and in vitro studies, subsequent use of animal experimental models is needed to further verify the sensitizing effect of the PDK inhibitor DCA on radiotherapy for gastric cancer. In addition, the structural modification and optimization of DCA to increase the affinity between DCA and PDK and to reduce the toxicity of DCA are also directions for future research.

5 Conclusion

The PDK inhibitor DCA inhibits the malignant progression of gastric cancer cells and modulates the radiotherapy resistance of gastric cancer cells, which provides a new idea for sensitization to radiotherapy in gastric cancer.

Acknowledgements None

Disclosure All authors have no conflicts of interest or financial ties to disclose.

Author contributions Qi Zhang:Responsible for research design, experimental implementation, data analysis and writing the first draft of the paper. Wanjia Qiao:Participate in research design, assist in experimental implementation and data analysis, and be responsible for the revision and finalization of the final version. Experimental implementation and data collection Xiaoyu Liu and Jun Lu:Responsible for statistical analysis, participate in data interpretation and result discussion. Farooq Benish:Responsible for chart making and data visualization, and assisting in data analysis. Xiaojun Liu and Shuping Li:As the project leader, he provides guidance on the overall research direction, supervises the research progress, and participates in the revision and review of papers. All authors have read and endorsed the final manuscript and are responsible for the accuracy and completeness of the findings. The authors declare no conflicts of interest.

Funding Non-profitCentral Research instituteFund of Chinese Academy of Medical Science (No.NLDTG2020018); Gansu Provincial People's Hospital Intramural Research Fund Project: (20GSSY1-24) (21GSSYA-2).

Data availability 1. The Linked Omics database (<http://www.linkedomics.org/login.php>) contains 32 cancer types in TCGA for gene enrichment analysis. The following parameters were set here: search dataset (RNA-seq data type, HiSeq RNA platform), search dataset attributes (PDK1), target dataset (RNA-seq data type, HiSeq RNA platform), and statistical method (Spearman correlation test). Gene Ontology (GO) and Kyoto Encyclopedia of Genes and Genomes (KEGG) analyses were performed using the Gene Set Enrichment Analysis (GSEA) functional module, with 0.05 set as the P-value threshold, and Spearman correlation tests were used for the The results were statistically analyzed. 2. STRING (<https://string-db.org/>) is an online open access bioinformatics analysis database that probes protein interactions. Set Protein Name: PDK1, Organization: Homo sapiens for protein interaction analysis of PDK1. The datasets and websites mentioned above are publicly available. The corresponding data and information can be accessed by visiting the respective websites or databases. The data generated in this study are included in the graphs or tables in this paper, which can be obtained from the corresponding author.

Declarations

Ethics approval and consent to participate The privacy and personal information of all participants were strictly protected to ensure that they were not disclosed during and after the study. Data collection, processing and analysis in this study followed the principle of integrity in

scientific research to ensure the authenticity, accuracy and completeness of the data. No manipulation or tampering that could distort the results of the study was performed during data analysis. This study has been conducted in strict accordance with the relevant ethical norms and standards, and has been formally approved by the Ethics Committee of Shanghai Vio Biotechnology Company under the approval number SHLS-BA-22101102.

Consent for publication All patients who participated in this study voluntarily signed an informed consent form and agreed to publication after being fully informed about the purpose of the study, the methodology, and the possible risks and benefits.

Competing interests The authors declare no competing interests.

Open Access This article is licensed under a Creative Commons Attribution-NonCommercial-NoDerivatives 4.0 International License, which permits any non-commercial use, sharing, distribution and reproduction in any medium or format, as long as you give appropriate credit to the original author(s) and the source, provide a link to the Creative Commons licence, and indicate if you modified the licensed material. You do not have permission under this licence to share adapted material derived from this article or parts of it. The images or other third party material in this article are included in the article's Creative Commons licence, unless indicated otherwise in a credit line to the material. If material is not included in the article's Creative Commons licence and your intended use is not permitted by statutory regulation or exceeds the permitted use, you will need to obtain permission directly from the copyright holder. To view a copy of this licence, visit <http://creativecommons.org/licenses/by-nc-nd/4.0/>.

References

1. Li P, Li Z, Linghu E, et al. Chinese national clinical practice guidelines on the prevention, diagnosis, and treatment of early gastric cancer. *Chin Med J*. 2024;137(8):887–908. <https://doi.org/10.1097/CM9.00000000000003101>.
2. Reynolds JV, Cowzer D, Janjigian YY. Should chemoradiotherapy be standard to maximise cure in localised gastro-oesophageal cancer? *Lancet Oncol*. 2022;23(7):847–9. [https://doi.org/10.1016/S1470-2045\(21\)00753-1](https://doi.org/10.1016/S1470-2045(21)00753-1).
3. Gu H, Huang T, Shen Y, et al. Reactive oxygen species-mediated tumor microenvironment transformation: the mechanism of radioresistant gastric cancer. *Oxid Med Cell Longev*. 2018;2018:5801209. <https://doi.org/10.1155/2018/5801209>.
4. Vaupel P, Multhoff G. Revisiting the Warburg effect: historical dogma versus current understanding. *J Physiol*. 2021;599(6):1745–57. <https://doi.org/10.1113/JP278810>.
5. Zhao M, Wei F, Sun G, et al. Natural compounds targeting glycolysis as promising therapeutics for gastric cancer: a review. *Front Pharmacol*. 2022;13:1004383. <https://doi.org/10.3389/fphar.2022.1004383>.
6. Wang X, Perez E, Liu R, et al. Pyruvate protects mitochondria from oxidative stress in human neuroblastoma SK-N-SH cells. *Brain Res*. 2007;1132(1):1–9. <https://doi.org/10.1016/j.brainres.2006.11.032>.
7. Liu KX, Everdell E, Pal S, et al. Harnessing lactate metabolism for radiosensitization. *Front Oncol*. 2021;11:672339. <https://doi.org/10.3389/fonc.2021.672339>.
8. Bhatt AN, Chauhan A, Khanna S, et al. Transient elevation of glycolysis confers radio-resistance by facilitating DNA repair in cells. *BMC Cancer*. 2015;15:335. <https://doi.org/10.1186/s12885-015-1368-9>.
9. Hirschhaeuser F, Sattler UGA, Mueller-Klieser W. Lactate: a metabolic key player in cancer. *Cancer Res*. 2011;71(22):6921–5. <https://doi.org/10.1158/0008-5472.CAN-11-1457>.
10. Sun L, Moritake T, Ito K, et al. Metabolic analysis of radioresistant medulloblastoma stem-like clones and potential therapeutic targets. *PLoS ONE*. 2017;12(4):e0176162. <https://doi.org/10.1371/journal.pone.0176162>.
11. Shen H, Hau E, Joshi S, et al. Sensitization of glioblastoma cells to irradiation by modulating the glucose metabolism. *Mol Cancer Ther*. 2015;14(8):1794–804. <https://doi.org/10.1158/1535-7163.MCT-15-0247>.
12. Cairns RA, Papandreou I, Suthphin PD, et al. Metabolic targeting of hypoxia and HIF1 in solid tumors can enhance cytotoxic chemotherapy. *Proc Natl Acad Sci U S A*. 2007;104(22):9445–50. <https://doi.org/10.1073/pnas.0611662104>.
13. De Mey S, Dufait I, Jiang H, et al. Dichloroacetate radiosensitizes hypoxic breast cancer cells. *Int J Mol Sci*. 2020;21(24):9367. <https://doi.org/10.3390/ijms21249367>.
14. Zwicker F, Kirsner A, Peschke P, et al. Dichloroacetate induces tumor-specific radiosensitivity in vitro but attenuates radiation-induced tumor growth delay in vivo. *Strahlenther Onkol*. 2013;189(8):684–92. <https://doi.org/10.1007/s00066-013-0354-x>.
15. Cao W, Yacoub S, Shiverick KT, et al. Dichloroacetate (DCA) sensitizes both wild-type and over expressing Bcl-2 prostate cancer cells in vitro to radiation. *Prostate*. 2008;68(11):1223–31. <https://doi.org/10.1002/pros.20788>.
16. Dong G, Chen Q, Jiang F, et al. Diisopropylamine dichloroacetate enhances radiosensitization in esophageal squamous cell carcinoma by increasing mitochondria-derived reactive oxygen species levels. *Oncotarget*. 2016;7(42):68170–8. <https://doi.org/10.18632/oncotarget.11906>.
17. Kim HS, Kim SC, Kim SJ, et al. Identification of a radiosensitivity signature using integrative metaanalysis of published microarray data for NCI-60 cancer cells. *BMC Genom*. 2012;13:348. <https://doi.org/10.1186/1471-2164-13-348>.
18. Wanotayan R, Chousangstorn K, Petisiwaweth P, et al. A deep learning model (FociRad) for automated detection of γ-H2AX foci and radiation dose estimation. *Sci Rep*. 2022;12(1):5527. <https://doi.org/10.1038/s41598-022-09180-2>.
19. Anwar S, Shamsi A, Mohammad T, et al. Targeting pyruvate dehydrogenase kinase signaling in the development of effective cancer therapy. *Biochim Biophys Acta Rev Cancer*. 2021;1876(1):188568. <https://doi.org/10.1016/j.bbcan.2021.188568>.
20. Hur H, Xuan Y, Kim YB, et al. Expression of pyruvate dehydrogenase kinase-1 in gastric cancer as a potential therapeutic target. *Int J Oncol*. 2013;42(1):44–54. <https://doi.org/10.3892/ijo.2012.1687>.
21. Stacpoole PW, Kerr DS, Barnes C, et al. Controlled clinical trial of dichloroacetate for treatment of congenital lactic acidosis in children. *Pediatrics*. 2006;117(5):1519–31. <https://doi.org/10.1542/peds.2005-1226>.

22. Tataranni T, Piccoli C. Dichloroacetate (DCA) and cancer: an overview towards clinical applications. *Oxid Med Cell Longev*. 2019;2019:8201079. <https://doi.org/10.1155/2019/8201079>.
23. Zhou L, Liu L, Chai W, et al. Dichloroacetic acid upregulates apoptosis of ovarian cancer cells by regulating mitochondrial function. *Onco Targets Ther*. 2019;12:1729–39. <https://doi.org/10.2147/OTT.S194329>.
24. Kim TS, Lee M, Park M, et al. Metformin and dichloroacetate suppress proliferation of liver cancer cells by inhibiting mTOR complex 1. *Int J Mol Sci*. 2021;22(18):10027. <https://doi.org/10.3390/ijms221810027>.
25. Sampadi B, Vermeulen S, Mišović B, et al. Divergent molecular and cellular responses to low and high-dose ionizing radiation. *Cells*. 2022;11(23):3794. <https://doi.org/10.3390/cells11233794>.
26. Raavi V, Perumal V, Paul SFD. Potential application of γ -H2AX as a biodosimetry tool for radiation triage. *Mutat Res Rev Mutat Res*. 2021;787:108350. <https://doi.org/10.1016/j.mrrev.2020.108350>.
27. Latocha M, Żyrek L. Anti-cancer properties of dichloroacetate. *Pol Merkuri Lekarski*. 2022;50(296):145–7.
28. Ippolito L, Morandi A, Giannoni E, et al. Lactate: a metabolic driver in the tumour landscape. *Trends Biochem Sci*. 2019;44(2):153–66. <https://doi.org/10.1016/j.tibs.2018.10.011>.
29. Grotius J, Dittfeld C, Huether M, et al. Impact of exogenous lactate on survival and radioresponse of carcinoma cells in vitro. *Int J Radiat Biol*. 2009;85(11):989–1001. <https://doi.org/10.3109/09553000903242156>.
30. Sattler UGA, Meyer SS, Quennet V, et al. Glycolytic metabolism and tumour response to fractionated irradiation. *Radiother Oncol*. 2010;94(1):102–9. <https://doi.org/10.1016/j.radonc.2009.11.007>.
31. Farhood B, Ashrafizadeh M, Khodamoradi E, et al. Targeting of cellular redox metabolism for mitigation of radiation injury. *Life Sci*. 2020;250:117570. <https://doi.org/10.1016/j.lfs.2020.117570>.
32. Averbek D, Rodriguez-Lafrasse C. Role of mitochondria in radiation responses: epigenetic, metabolic, and signaling impacts. *Int J Mol Sci*. 2021;22(20):11047. <https://doi.org/10.3390/ijms222011047>.
33. Liu X, Xi X, Xu S, et al. Targeting T cell exhaustion: emerging strategies in non-small cell lung cancer. *Front Immunol*. 2024;15:1507501. <https://doi.org/10.3389/fimmu.2024.1507501>.
34. Xu S, Lu Z. Exploring FNDC4 as a biomarker for prognosis and immunotherapy response in lung adenocarcinoma. *Asian J Surg*. 2024;S1015–9584(24):02098. <https://doi.org/10.1016/j.asjsur.2024.09.054>.
35. Xuan Y, Hur H, Ham I-H, et al. Dichloroacetate attenuates hypoxia-induced resistance to 5-fluorouracil in gastric cancer through the regulation of glucose metabolism. *Exp Cell Res*. 2014;321(2):219–30. <https://doi.org/10.1016/j.yexcr.2013.12.009>.
36. Ma Y, Zhang X, Han X, et al. PDK1 regulates the progression of esophageal squamous cell carcinoma through metabolic reprogramming. *Mol Carcinog*. 2023;62(6):866–81. <https://doi.org/10.1002/mc.23531>.
37. Sun L, Jiang Y, Yan X, et al. Dichloroacetate enhances the anti-tumor effect of sorafenib via modulating the ROS-JNK-Mcl-1 pathway in liver cancer cells. *Exp Cell Res*. 2021;406(1):112755. <https://doi.org/10.1016/j.yexcr.2021.112755>.
38. Babu E, Ramachandran S, Coothankandaswamy V, et al. Role of SLC5A8, a plasma membrane transporter and a tumor suppressor, in the antitumor activity of dichloroacetate. *Oncogene*. 2011;30(38):4026–37. <https://doi.org/10.1038/onc.2011.113>.
39. Calcutt NA, Lopez VL, Bautista AD, et al. Peripheral neuropathy in rats exposed to dichloroacetate. *J Neuropathol Exp Neurol*. 2009;68(9):985–93. <https://doi.org/10.1097/NEN.0b013e3181b40217>.

Publisher's Note Springer Nature remains neutral with regard to jurisdictional claims in published maps and institutional affiliations.